ASTRONOMY & ASTROPHYSICS
SUPPLEMENT SERIES

Astron. Astrophys. Suppl. Ser. **134**, 483–487 (1999)

The Hamburg Quasar Survey⋆,⋆⋆,⋆⋆⋆

III. Further new bright quasars

H.-J. Hagen, D. Engels, and D. Reimers

Hamburger Sternwarte, Gojenbergsweg 112, D-21029 Hamburg, Germany
Internet: www.hs.uni-hamburg.de

Received July 9; accepted September 3, 1998

Abstract. We present a further list of 274 bright QSOs, 106 (195) of which have $B \lesssim 17$ (17.5), selected semiautomatically from objective prism plates taken with the Calar Alto 80 cm Schmidt telescope. All QSOs have been confirmed by follow-up spectroscopy and we display their flux-calibrated spectra. We also discuss the completeness of our search technique and demonstrate that for $0.1 \leq z < 3.2$ and $B \leq 17$ we have been able to recover roughly 85% of known QSOs; 10% were lost due to overlaps while 5% were lost during the selection process. In particular the bright $z \geq 2$ QSOs (17 with $B \lesssim 17$) are potential targets for follow-up spectroscopy both at high-resolution from the ground and in the ultraviolet from space.

Key words: surveys — quasars: general

1. Introduction

The search for bright quasars ($B \leq 17.0$) has ever been a challenge for all surveys because of their low surface density. On a typical Schmidt field of 25 deg^2 about 5 bright quasars are expected to be found (Hewett et al. 1995; Köhler et al. 1997) among 30−90 000 other objects, thus demanding a large coverage of the sky with plates and an efficient selection technique to find a sizeable fraction of such QSOs. The Hamburg Quasar Survey (HQS, Hagen et al. 1995; hereafter Paper I) covers $\approx 13\,600$ deg^2 of the northern sky ($\delta > 0°$) at galactic latitudes $\mid b \mid > 20°$ with digitized objective prism plates, allowing a comprehensive search for these QSOs. On the base of the above mentioned surface densities and taking into account galactic absorption, roughly $10^3\,B \lesssim 17.0$ QSOs are expected in this area, while the most recent QSO catalogue (Véron-Cetty & Véron 1996) lists about 500 QSOs with $B \leq 17.0$ in the same area.

At an even brighter level ($V \approx 16$) the Palomar-Green-Survey (Green et al. 1986; Schmidt & Green 1983) has already discovered the vast majority of QSOs in the HQS area, although no attempt has been made yet to verify its completeness since then (but see Goldschmidt et al. 1992; Savage et al. 1993; Köhler et al. 1997). This survey was restricted to redshifts $z \leq 2.2$ due to its selection technique, leaving the surface density of high-redshift $z > 2.2$ QSOs at $B \leq 17.0$ unsettled (see Hartwick & Schade 1990). An extrapolation from fainter levels to $B \leq 17.0$ predicts a number of the order of 10^2 QSOs in the HQS area, while the Véron-Cetty & Véron catalogue lists 34 so far – including 4 HQS QSOs already published.

Summarizing we expect to at least double the number of bright $z \geq 2$ QSOs in the survey area. The bright high-redshift QSOs from the Hamburg Quasar Survey published so far (Reimers et al. 1989; Hagen et al. 1992; Reimers et al. 1995) have been the source of considerable progress in our understanding of the intergalactic medium via high-resolution, high S/N optical spectra (metal lines: Tripp et al. 1996, 1997; Lyα forest: Kirkman & Tytler 1997) and by means of UV spectra using HST (HeI: Reimers & Vogel 1993; UV high ionization resonance lines: Reimers et al. 1992; Vogel & Reimers 1995) or the Hopkins Ultraviolet Tetelescope (HUT) (HeII: Davidsen et al. 1996).

Send offprint requests to: H.-J. Hagen
e-mail: hhagen@hs.uni-hamburg.de

⋆ Based on observations obtained at the German-Spanish Astronomical Center, Calar Alto, Spain, operated by the Max-Planck-Institut für Astronomie, Heidelberg, jointly with the Spanish National Commission for Astronomy and at the European Southern Observatory, La Silla, Chile.

⋆⋆ Table 3 is only available in electronic form at the CDS via anonymous ftp to cdsarc.u-strasbg.fr (130.79.128.5) or via http://cdsweb.u-strasbg.fr/Abstract.html

⋆⋆⋆ Figure 3 is only available at the journal, http://www.edpsciences.com

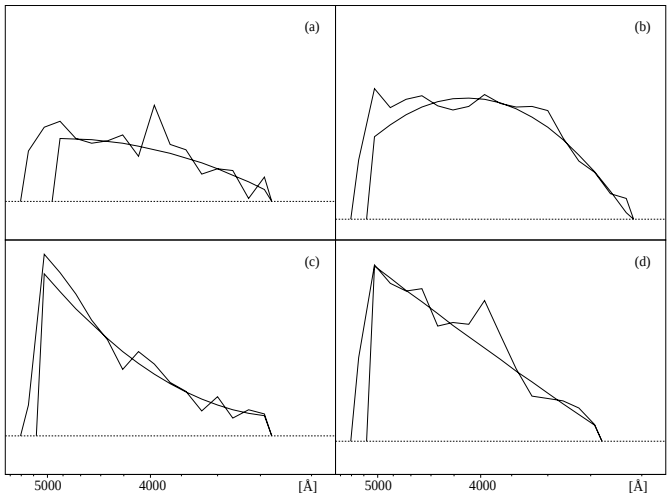

Fig. 1. Examples of lrs-spectra with continuum fit. **a)** QSO HS 0948+4735, displaying a CIV emission line at ≈ 4000 Å. **b)** QSO SBS 0946+50 at $z = 1.22$ without prominent emission line, **c)** and **d)** random stellar spectra

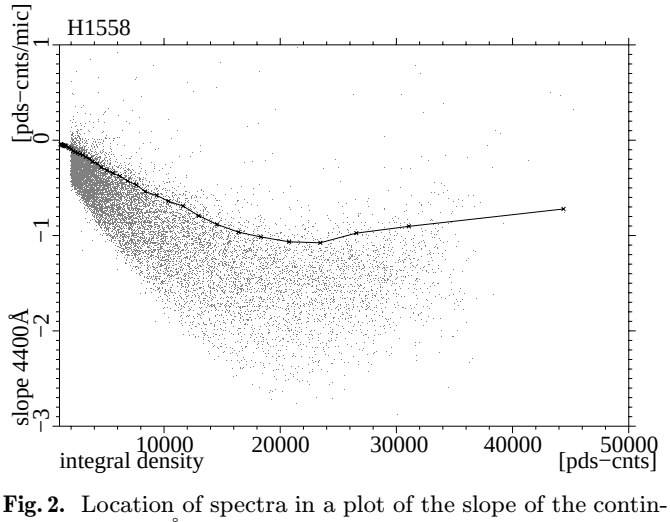

Fig. 2. Location of spectra in a plot of the slope of the continuum Σ at 4400 Å against integral density. The density is given in internal machine units (pds-counts). All spectra above the plotted dividing line (see text) are selected

In this paper we present a further list of bright, spectroscopically verified QSOs. While this list is not a complete sample, we briefly estimate the potential completeness of our survey. Details on the Schmidt observations and the digitization method were described in Paper I. A first list of QSOs found during the development phase of the search technic was published in Engels et al. (1998).

2. Selection criteria for QSO candidates

The objective prism plates are scanned with a PDS 1010G microdensitometer in a low-resolution mode (see Paper I). After on-line background reduction and object recognition, the low-resolution density spectra are stored on magneto-optical disc. At a given brightness of an object, its density spectrum has basically a triangular shape, which peaks close to the steep emulsion cut-off at $\lambda\,5400$ Å and declines gradually in density towards the ultraviolet border at $\lambda\,3400$ Å. This characteristic shape is a result of the convolution of the compressed wavelength scale close to the cut-off, which is caused by the non-linear dispersion, and the (usually) rising spectral energy distribution of the objects. In Fig. 1 a few examples are given.

The density spectra are characterized by several parameters as are their spectral length, amplitude, integral density, center of gravity, slope of the spectral density etc. In principle, a multi-parameter space can be constructed in which most of the spectra will occupy a particular volume, the main locus. As quasar spectra often show an ultraviolet excess and possess emission lines, their appearance will differ from those of most of the stars, and they are expected to be found in the multi-parameter space outside the main locus. To ease the handling of the data a principal component analysis can be performed to reduce the dimensions of the parameter space (Francis et al. 1992). In practice, however, objective prism QSO surveys used two-parameter spaces, with the most efficient selection parameter(s) determined by experiment (Hewett et al. 1995; Wisotzki et al. 1996). This approach is also followed by the HQS, with the slope of the spectral density Σ used as the selection parameter. For its definition the spectra are fitted with a polynomial of 2nd degree with Σ being the slope of this fit at 4400 Å. The fit procedure is iterative omitting density values of individual pixels deviating significantly from the density predicted by the previous fit. The influence of strong emission lines and crippled pixels on the determination of the continuum slope is therefore greatly diminished. Examples for individual fits are given in Fig. 1.

Blue spectra are selected by the determination of a dividing line in the two-parameter space defined by Σ and the integral density. The distribution of spectra in this space is non-linear due to spectral variations of the characteristic curve. A typical distribution is shown in Fig. 2, where the distribution of Σ as a function of the integral density for all spectra of the plate H1558 is plotted. Spectra are flat for weak and very great densities, and show the steepest slopes in the linear part of the characteristic curve. The reason for this behaviour are changes in the contrast in sensitivity of the plate across the wavelength region $\lambda\,3400 - 5400$ Å. The contrast first increases as a function of the absolute density, which means that the density spectra of faint objects all have a similar flat slope while the mean slope steepens with increasing absolute density. With further increase of the absolute density, the spectra saturate starting at the red cut-off resulting in a decrease in the contrast and hence in a re-flattening of the spectra. The result is a curved distribution as shown in Fig. 2.

The dividing line to select blue spectra has to be determined in the curved distribution of the chosen two-parameter space, and the determination has to be made individually for each plate, as its locus is also a function of the shape of the characteristic curve of the plate. For each plate spectra are collected into intervals of integral density containing 500 spectra. The widths of the intervals are therefore varying, being small at low densities and increasing towards higher densities. In each interval a limiting slope is determined which separates the bluest spectra from the rest. Depending on the width of the interval the fraction of the selected spectra decreases with increasing integral density, starting with $\approx 20\%$ for the lowest density levels and decreasing to $\approx 5\%$ for high densities. This accounts for the varying effectiveness of our selection criterion with integral density. The dividing line is finally obtained by interpolation of the limiting slope values.

The selection criterion fails for the lowest and highest density levels. Thus spectra with integral densities ≤ 2000 and $\gtrsim 40000 - 50000$ are discarded. The lower limit corresponds to our completeness limit for the extraction of spectra by our digitization technique (see Paper I), making selection of blue spectra below this limit less reliable anyway.

The selected blue spectra are rescanned individually with full resolution and sampling, and are classified visually on a graphics display. The digitized direct plates are used to recognize overlaps, to probe for extended images, and to determine coordinates. Objects are discarded as QSO candidates, if one of the following cases applies:

- Absorption features, such as the G-Band at 4300 Å and the Ca H+K lines qualify the spectrum as stellar,
- Balmer absorption lines qualify the spectrum as stellar with high effective temperature,
- an extended image on the direct plate and a strong emission line close to the green head of the spectrum ($\lambda \approx 5400$ Å) suggests the presence of a strong $\lambda\,5007$ Å O[III] emission line, qualifying the correspondent object as a narrow-emission line galaxy (Vogel et al. 1993).

The remaining objects are divided into two categories. In spectra of primary candidates broad emission lines must be detectable while spectra of secondary candidates are featureless and not distinguishable from hot star spectra with small absorption lines which cannot be resolved in our density data.

3. Completeness of the selection method

The spectral energy distribution of QSOs in the optical wavelength regime is dominated by an ultraviolet excess and broad emission lines. Depending on redshift, one or the other feature is more prominent, and therefore the reliability to select QSOs with a given selection criterion varies with redshift. Quasars are not selected if the parameters of their density spectra are too similar to those of stars, unless the parameter space accepted for selection is made rather broad. This may lead to a contamination of the QSO candidate sample with stars, decreasing the effectiveness of the selection process to an unacceptable low level. Thus, completeness is traded off for efficiency and surveys have to emphasize one of the aspects, depending on their primary aims.

In the present stage the selection and the priorities for follow-up spectroscopy of the HQS emphasize effectiveness, motivated by the aim to find new bright high-redshift quasars. However, due to the classification strategy to exclude as quasar candidates only those objects, which can be classified positively as stars or as non-AGN-galaxies, the possibility to determine the survey selection function is preserved. The survey selection function determines the reliabilitity of a selection procedure as a function of brightness, redshift and spectral energy distribution of quasars (Hewett & Foltz 1994). While follow-up spectroscopy is made currently mostly of objects classified as prime QSO candidates, the determination of the selection function would require spectroscopy of the secondary candidates as well. Their number is a factor of ≈ 3 greater than the number of QSO candidates, making such an undertaking feasible only on a restricted part of the sky covered by the HQS.

Our selection process of quasar candidates is semi-automated. In the first step an automated selection is done by using the spectral slope as discriminating parameter. In the second step a subjective selection is made based on the visual classification of the high-resolution density spectra. For both steps the reliability of the selection has to be evaluated separately. For the search of bright high-redshift QSOs the first step is the critical one, because mostly the broad emission Ly-α line makes the density spectra so outstanding that they will not be missed visually, except that the spectra are distorted by overlaps.

To check the reliability of our candidate selection our present digitized database of 418 processed fields was correlated with the quasar catalogue of Véron-Cetty & Véron (1996). We compiled all Veron catalogue entries that have magnitudes less than 17 and a redshift from 0.1 to 3.2. The smaller redshifts were left out because bright extended objects often show crippled digitized LRS spectra allowing no reliable classification. We found 370 entries which we searched for among our digitized LRS spectra up to a maximum distance from their catalogue position. 5% could not be found due to overlapping spectra and another 5% could not be found on both the direct and the prism plate, possibly due to incorrect brightnesses or positions in the catalogue. Discarding all objects with a B magnitude of greater value than 17 on our Schmidt plates resulted in the final sample of 189 QSOs. In the first automatical slope dependent step of the selection process 1 QSO was not selected due to overlapping spectra. From the automatically

Table 1. Epoch, spectrograph, and achieved spectral resolution of follow-up spectroscopic data. Except of run 1 at the 3.6 m-telescope of ESO and run 9 at the 3.5 m telescope on Calar Alto all data were obtained with the 2.2 m-telescope on Calar Alto

Epoch		Spectrograph	Res. [Å/pix.]	No.
Aug. 5 - 8	1992	EFOSC1	6.4	1
Aug. 7 - 11	1992	B&C	5.2	2
Mar. 9 - 14	1993	B&C	10.3	3
Aug. 5 - 9	1993	B&C	31.2	4
Feb. 18 - 23	1994	B&C	30.3	5
Sep. 6 - 8	1994	B&C	15.5	6
Mar. 14 - 16	1995	B&C	15.6	7
Aug. 25 - 28	1995	CAFOS	9.4	8
Mar. 20 - 22	1996	Focal Red.	3.3	9
Oct. 2 - 4	1996	CAFOS	9.8	10
Feb. 28 - Mar. 4	1997	CAFOS	9.8	11
Aug. 19 - 24	1997	CAFOS	9.7	12
Feb. 16 - 21	1998	CAFOS	9.7	13

selected 188 QSOs further 9 had overlapping spectra, and 8 were misclassified during the subsequently visual classification. Altogether, approximately 10% were lost due to overlaps on the Schmidt plates, and further 5% were misclassified during the interactive classification.

On the other hand the use of a compilation of QSOs drawn from many sources includes unknown biasing effects. For example, the parameter cube spanned by brightness, redshift and spectral slope is certainly not covered homogeneously. The number of objects is still too small for dividing the parameter cube into a large number of cells, inside which averaging over the properties of the plates (position on the characteristic curve, seeing effects etc.) would then be possible. Thus, at this stage it is not possible to determine the selection function for the full survey.

The use of the Véron-Cetty & Véron catalogue introduces possible biases of earlier surveys into the completeness test, as, e.g., the controversially discussed possibility that QSOs are hidden by dust will prevent selection by optical surveys because of the redness of their continuum (Webster et al. 1995; Boyle & di Matteo 1995). Summarizing, we consider the automatic selection using the continuum slope as insensible to losing bright quasars unless they have spectral slopes which cannot be distinguished from stars on objective-prism plates.

4. Follow-up spectroscopy

Candidates were verified by slit spectroscopy mainly with the 2.2 m telescope on Calar Alto, Spain, equipped with a Cassegrain Boller & Chivens spectrograph or since 1995 with the faint object spectrograph CAFOS. Some candidates were observed in August 1992 by N. Bade with ESO's EFOSC1 at the 3.6 m telescope on La Silla, Chile.

Table 2. QSOs with detectable neighbours on direct Schmidt plates

object	neighbour
HS 0042+3704	galaxy
HS 0423+0658	galaxy
HS 0808+1218	galaxy
HS 0855+7456	galaxy
HS 1016+2845	galaxy
HS 1121+2700	galaxy
HS 1125+2418	horizontal branch star
HS 1137+8003	galaxy
HS 1231+2519	2 galaxies ($z = 0.22$ and $z =?$)
HS 1414+2330	stellar
HS 1546+3903	galaxy
HS 2209+1914	galaxy

HS 0025+3047 was observed for a second time by W. Kollatschny from the Universitätssternwarte Göttingen with the 3.5 m telescope on Calar Alto equipped with the TWIN spectrograph because the resolution of our data had been too small to detect its narrow emission lines. Three further objects were observed as backup programme with the same telescope but equipped with the Focal Reducer in March 1996.

HS 1216+5031 was serendipitously detected during the observations of the double quasar HS 1216+5032 (Hagen et al. 1996). At a distance of $\approx 115''$ this high redshift quasar is located on the opposite side of the brighter component at such a position angle that all three objects are visible in one slit position of the spectrograph.

Flatfield correction and wavelength and flux calibration of the CCD data followed standard procedures (cf. Stickel et al. 1993). In Table 1 the epoch, used instruments, and the achieved resolution are listed for all observing runs.

For all objects finding charts in postscript format and FITS files of the slit spectra are available on our Web page http://www.hs.uni-hamburg.de.

For almost all objects with detectable neighbours on our direct Schmidt plates (distance $\lesssim 10''$) the spectrograph was rotated to get both spectra simultaneously. Table 2 lists these objects with the object type of their neighbours. Already published are HS 1216+5032 (Hagen et al. 1996) and HS 1543+5921 (Reimers & Hagen 1998).

Table 3 (available at the CDS) lists for all objects the position for equinox 2000.0 with an accuracy $\lesssim 2''$, the B magnitude obtained from the Schmidt plates with an accuracy $\lesssim 0.5$ (see Paper I), the redshift, and the number of the campaign of Table 1 in which the data were obtained. Calibrated flux data of the objects are shown in Fig. 3 (available in the on-line version of this paper). Absolute flux calibration cannot be provided due to varying weather conditions during the various observing runs.

5. Final remarks

The QSOs in Table 3 are in no respect, neither redshift nor brightness, a complete sample. They represent a further preliminary list of bright QSOs for which low resolution follow-up spectroscopy has been completed. Publication at this stage appears appropriate since in particular the bright high-redshift QSOs are potential targets for present (HST) and future (FUSE) space missions as well as for high-resolution spectroscopy from the ground.

Acknowledgements. This research has made use of the NASA/IPAC extragalactic database (NED) which is operated by the Jet Propulsion Laboratory, Caltech, under contract with the NASA (U.S.A.). We like to acknowledge the generous support of the Deutsche Forschungsgemeinschaft through grants Re 353/11-1,2,3,4,5 and Re 353/22-1,2,3.

References

Boyle B.J., di Matteo T., 1995, MNRAS 277, L63
Davidsen A.F., Kriss G.A., Zheng W., 1996, Nat 380, 47
Engels D., Hagen H.-J., Cordis L., et al., 1998, A&AS 128, 507
Francis P.J., Hewett P.C., Foltz C.B., Chaffee F.H., 1992, ApJ 398, 476
Goldschmidt P., Miller L., La Franca F., Christiani S., 1992, MNRAS 256, 65p
Green R.F., Schmidt M., Liebert J., 1986, ApJS 61, 305
Hagen H.-J., Cordis L., Engels D., et al., 1992, A&A 253, L5
Hagen H.-J., Groote D., Engels D., Reimers D., 1995, A&AS 111, 195 (Paper I)
Hagen H.-J., Hopp U., Engels D., Reimers D., 1996, A&A 308, L25
Hartwick F.D.A., Schade D., 1990, ARA&A 28, 437
Hewett P.C., Foltz C.B., 1994, PASP 106, 113
Hewett P.C., Foltz C.B., Chaffee F.H., 1995, AJ 109, 1498
Köhler T., Groote D., Reimers D., Wisotzki L., 1997, A&A 325, 502
Reimers D., Hagen H.-J., 1998, A&A 329, L25
Reimers D., Vogel S., 1993, A&A 276, L13
Reimers D., Clavel J., Groote D., et al., 1989, A&A 218, 71
Reimers D., Vogel S., Hagen H.-J., et al., 1992, Nat 360, 561
Reimers D., Rodriguez-Pascual P., Hagen H.-J., Wisotzki L., 1995, A&A 293, L 21
Savage A., Cannon R.D., Stobie R.S., et al., 1993, Proc. ASA 10, 265
Schmidt M., Green R.F., 1983, ApJ 269, 352
Stickel M., Fried J.W., Kühr H., 1993, A&AS 98, 393
Tripp T.M., Lu L., Savage B.D., 1996, ApJS 102, 239
Tripp T.M., Lu L., Savage B.D., 1997, ApJS 112, 1
Kirkman D., Tytler D., 1997, ApJ 484, 672
Véron-Cetty M.P., Véron P., 1996, ESO Scientific Report 17
Vogel S., Reimers D., 1995, A&A 294, 377
Vogel S., Engels D., Hagen H.-J., et al., 1993, A&AS 98, 193
Webster R.L., Francis P.J., Peterson B.A., et al., 1995, Nat 375, 469
Wisotzki L., Köhler T., Groote D., Reimers D., 1996, A&AS 115, 227